

Full Subunit Coverage Liquid Chromatography Electrospray Ionization Mass Spectrometry (LCMS+) of an Oligomeric Membrane Protein

CYTOCHROME *b₆f* COMPLEX FROM SPINACH AND THE CYANOBACTERIUM *MASTIGOCLADUS LAMINOSUS*^{†§}

Julian P. Whitelegge^{‡§}, Huamin Zhang[¶], Rodrigo Aguilera[‡], Ross M. Taylor^{||}, and William A. Cramer[¶]

Highly active cytochrome *b₆f* complexes from spinach and the cyanobacterium *Mastigocladus laminosus* have been analyzed by liquid chromatography with electrospray ionization mass spectrometry (LCMS+). Both size-exclusion and reverse-phase separations were used to separate protein subunits allowing measurement of their molecular masses to an accuracy exceeding 0.01% (± 3 Da at 30,000 Da). The products of *petA*, *petB*, *petC*, *petD*, *petG*, *petL*, *petM*, and *petN* were detected in complexes from both spinach and *M. laminosus*, while the spinach complex also contained ferredoxin-NADP⁺ oxidoreductase (Zhang, H., Whitelegge, J. P., and Cramer, W. A. (2001) Flavonucleotide:ferredoxin reductase is a subunit of the plant cytochrome *b₆f* complex. *J. Biol. Chem.* 276, 38159–38165). While the measured masses of PetC and PetD (18935.8 and 17311.8 Da, respectively) from spinach are consistent with the published primary structure, the measured masses of cytochrome *f* (31934.7 Da, PetA) and cytochrome *b* (24886.9 Da, PetB) modestly deviate from values calculated based upon genomic sequence and known post-translational modifications. The low molecular weight protein subunits have been sequenced using tandem mass spectrometry (MSMS) without prior cleavage. Sequences derived from the MSMS spectra of these intact membrane proteins in the range of 3.2–4.2 kDa were compared with translations of genomic DNA sequence where available. Products of the spinach chloroplast genome, PetG, PetL, and PetN, all retained their initiating formylmethionine, while the nuclear encoded PetM was cleaved after import from the cytoplasm. While the sequences of PetG and PetN revealed no discrepancy with translations of the spinach chloroplast genome, Phe was detected at position 2 of PetL. The spinach chloroplast genome reports a codon for Ser at position 2 imply-

ing the presence of a DNA sequencing error or a previously undiscovered RNA editing event. Clearly, complete annotation of genomic data requires detailed expression measurements of primary structure by mass spectrometry. Full subunit coverage of an oligomeric intrinsic membrane protein complex by LCMS+ presents a new facet to intact mass proteomics. *Molecular & Cellular Proteomics* 1:816–827, 2002.

Mass spectrometry (MS)¹ has revolutionized the biological sciences since the development of matrix-assisted laser desorption ionization (MALDI) (1) and electrospray ionization (ESI) (2) in the late eighties (3), fertilizing the emergence of a new discipline called proteomics. Biological macromolecules are now mass-measured with great accuracy, and highly resolved spectra reveal subtle molecular heterogeneity. In fact, a mass spectrum of an intact protein is an essential piece of proteomic information that defines the native covalent profile of the product of a gene and its associated heterogeneity (4). For intact proteins, ESI-MS provides superior accuracy (within 0.01% error) and resolution, while MALDI is more sensitive and more tolerant of extreme heterogeneity and complex mixtures. Although intrinsic membrane proteins have been traditionally regarded as problematic, a suite of techniques has been developed that allows routine ESI-MS of numerous examples with up to 15 transmembrane helices (4–8). Although proteomics has largely been fueled by utilization of mass spectrometry to *identify* proteins, based upon mass and sequence analysis of small peptides derived from the parent protein, it is now possible to include intact mass measurements as an integral part of proteomics (*intact mass proteomics*).

An isolated fully active protein complex is especially useful in proteomics because it defines the functional unit and the

From [‡]The Pasarow Mass Spectrometry Laboratory, Departments of Psychiatry and Biobehavioral Sciences, Chemistry and Biochemistry, and the Neuropsychiatric Institute, University of California, Los Angeles, California 90095, the [¶]Department of Biological Sciences, Purdue University, West Lafayette, Indiana 47907, and the ^{||}Department of Microbiology, Montana State University, Bozeman, Montana 59717

Received, August 7, 2002, and in revised form, October 5, 2002
Published, MCP Papers in Press, October 11, 2002, DOI 10.1074/mcp.M200045-MCP200

¹ The abbreviations used are: MS, mass spectrometry; MALDI, matrix-assisted laser desorption ionization; ESI, electrospray ionization; FNR, ferredoxin-NADP⁺ oxidoreductase; LCMS+, liquid chromatography with mass spectrometry and fraction collection; MSMS, tandem mass spectrometry; SEC, size-exclusion chromatography; PS, photosystem; TOF, time-of-flight; HPLC, high pressure liquid chromatography.

structural genes that interact to provide this functionality, although other gene products may of course be involved for successful assembly and regulation. Consequently, intrinsic membrane protein complexes have been previously targeted for analysis by mass spectrometry with some success. MALDI was used successfully for analysis of cytochrome bo_3 (4 subunits) and cytochrome bd (2 subunits) from *Escherichia coli* as well as the bc_1 complex (3 subunits) and cytochrome c oxidase (3 subunits) from *Rhodobacter sphaeroides* (9). However, lower accuracy and resolution in MALDI of larger proteins lessens the value of these analyses compared with ESI, although it is noted that some membrane proteins have recently been analyzed with improved accuracy by MALDI (10). ESI interfaced to HPLC (LCMS) was applied to bovine cytochrome bc_1 complex, but not all subunits were detected (11). Photosystem 2 (PS2) reaction-center subcomplexes have been successfully analyzed by ESI (4, 12–14) as have appressed thylakoid membrane subfractions that include the PS2 dimer and associated light-harvesting complex polypeptides (8), although a systematic, comprehensive examination of the native PS2 dimer has yet to be described. Toward the goal of complete description of an oligomeric intrinsic membrane protein complex, a number of techniques were used to fully characterize highly active preparations of cytochrome b_6f complex, including the cytochrome b_6 (PetB) and subunit IV (PetD) subunits that have a total of seven transmembrane helices.

The cytochrome b_6f complex provides the electronic connection between the two reaction centers, photosystem 2 and 1, of oxygenic photosynthesis and, by oxidizing the lipophilic plastoquinol and transferring the resulting protons to the electrochemically positive side of the membrane, also contributes to the generation of the transmembrane proton electrochemical potential that drives ATP synthesis (15). This function is analogous to that carried out by the cytochrome bc_1 complex of bacterial photosynthesis and the respiratory chain with which there are many closely similar features, including the redox cofactors and the cytochrome b polypeptide in the membrane core of the complexes (16). The b_6f complex contains at least four redox cofactors, the two b hemes, the heme of cytochrome f , and the high potential [2Fe-2S] cluster of the Rieske iron-sulfur protein and a fifth, the FAD moiety of the ferredoxin:NADP⁺ reductase in the b_6f complex from spinach (17) and presumably other plant sources. The latter cofactor has no analogue in the cytochrome bc_1 complex. The b_6f complex has been purified as a very active (>300 electrons/cytochrome f/s) dimer with eight and nine polypeptide subunits and a molecular weight of ~210,000 and 280,000, respectively, in the cyanobacterium *Mastigocladus laminosus* and spinach chloroplasts (with FNR) (17). Twenty-six transmembrane helices are predicted in the dimeric complex.

Two-dimensional crystals of the b_6f complex from the green alga *Chlamydomonas reinhardtii* have been obtained that provide maps to 8–9 Å (18, 19), and three-dimensional crystals of

the complex from the thermophilic cyanobacterium *M. laminosus* (20) have been obtained that diffract to <4 Å. The space group and unit cell dimensions have been determined.² High resolution (~1.8–1.9 Å) structures, which will facilitate the solving the structure of the complex, have previously been obtained of the lumen-side soluble domains of cytochrome f (21) and the Rieske iron-sulfur protein (22, 23) that constitute ~40% of its total mass. The high resolution structure of the soluble form of cytochrome f , which turns out to be completely different from cytochrome c_1 and a unique c -type cytochrome (24), has been obtained from plant chloroplasts (21), cyanobacteria (23), and green algae (26).

As part of an effort to better understand the structure and evolution of the b_6f complex a complete mass spectroscopic characterization of the b_6f complex isolated from spinach thylakoids and *M. laminosus* has been performed. This is the first complete mass spectroscopic characterization of an active, multiply oligomeric, integral membrane protein complex from more than one phylum, providing precise information about the detailed nature of the complex that has helped to catalyze the successful crystallization of the b_6f complex.

EXPERIMENTAL PROCEDURES

Preparation of the cytochrome b_6f complex from spinach chloroplasts and the thermophilic cyanobacterium *M. laminosus* and quantitation of polypeptide, heme content, and activity of the complex have been described (17). The electron transfer activity, from reduced decyl-plastoquinol to plastocyanin oxidized by ferricyanide, of the complex isolated from both sources was the same within experimental error, 250–350 electrons/cytochrome f/s , and the same as the activities measured *in situ* or *in vivo* (17). As noted previously, the absence of FNR in the cyanobacterial complex did not affect linear electron transfer (17).

Samples of isolated cytochrome b_6f complex were analyzed by liquid chromatography with mass spectrometry and fraction collection (LCMS+). Protein (200 μg) was precipitated with either chloroform/methanol or cold acetone. Precipitation at the interface of an aqueous chloroform/methanol phase separation (27) was as described previously (5). Precipitated proteins were recovered after removal of the aqueous phase and addition of methanol. Proteolipids (proteins with lipid-like properties) were isolated by recovery of the lower phase. Precipitated samples were dried at atmospheric pressure for 2 min (25 °C) and dissolved in 60% formic acid (100 μl) immediately prior to HPLC. Acetone precipitation was achieved by addition of 1 ml of 80% aqueous acetone (–20 °C), vigorous mixing for 1 min, and incubation for 30 min (–20 °C). Material was recovered by centrifugation (30 s at 10,000 × *g* in a microcentrifuge).

Size-exclusion Chromatography—SEC was performed in chloroform/methanol/1% aqueous formic acid (4:4:1, v/v) as described previously (5) using a Super SW2000 column (4.6 × 300 mm, Tosoh Biosep) at 250 μl/min (40 °C). Precipitated proteins were dissolved in 60% formic acid (or 70% acetic acid), or proteolipids in the lower phase were loaded using a 100-μl loop.

Reverse-phase Chromatography—Reverse-phase chromatography of intact intrinsic membrane proteins was performed as described previously (4) using a macroporous polymeric support (PLRP/S, 300 Å, 5 μm, 2 × 150 mm, Polymer Labs) at 100 μl/min

² H. Zhang, G. Kurisu, and W. A. Cramer, manuscript in preparation.

(40 °C). Alternatively, the column was previously equilibrated in 95% A, 5% B (A, 0.1% trifluoroacetic acid in water; B, 0.05% trifluoroacetic acid in acetonitrile/isopropanol (1:1)) and eluted with a compound linear gradient from 5% B at 5 min after injection, through 40% B at 30 min, and to 100% B at 150 min. The eluent was passed through a UV detector (280 nm).

LCMS+ — Fractions were collected concomitant with ESI-MS using a liquid-flow splitter inserted between the HPLC detector and mass spectrometer. A fused silica capillary was used to transfer liquid to the ESI source (50 cm) or fraction collector (25 cm). Fractions were collected into microcentrifuge tubes at 1-min intervals. For cyanogen bromide (CNBr) cleavage one-tenth volume of CNBr solution (1 g/ml in acetonitrile) was added to each fraction, and, after a 3-h incubation in the dark at room temperature, the sample was dried by centrifugal evaporation (SpeedVac, Savant). Peptides were dissolved in small volumes (5 μ l) of 70% acetic acid for MALDI-TOF.

Electrospray Ionization Mass Spectrometry—ESI-MS was performed as described previously (4) using a triple quadrupole instrument (API III, Applied Biosystems). Data were processed using MacSpec 3.3, Hypermass, or BioMultiview 1.3.1 software (Applied Biosystems). Tandem mass spectrometry (MSMS) was performed under standard conditions with orifice voltage and collision gas (99.999% argon) thickness to achieve 20–90% fragmentation of the parent ion. Spinach PetL and *M. lamosus* PetG and PetL sequences were obtained by analysis of fractions collected during reverse-phase LCMS+ using nanospray ESI-MSMS on a quadrupole time-of-flight mass spectrometer (Q-Star Pulsar, Applied Biosystems, equipped with Protana source).

MALDI time-of-flight (MALDI-TOF) was performed using a high performance UV laser time-of-flight mass spectrometer (Voyager DE-STR, Applied Biosystems) operated in reflector mode with internal calibration where possible. 0.5 μ l of a matrix solution (10 mg/ml α -cyano-4-hydroxycinnamic acid in 0.1% trifluoroacetic acid, 70% acetonitrile) was mixed with 0.3 μ l of an HPLC fraction collected during LCMS+ (stored at –20 °C).

RESULTS

Organic solvents were used to extract lipid and pigment molecules and precipitate the polypeptide subunits of the complex. Precipitation at the interface of a chloroform/methanol/water phase separation (27) was effective, although PetN and PetL partitioned into the lower chloroform-enriched phase and can thus be regarded as proteolipids. Consequently, more recent analyses used precipitation in 80% acetone at –20 °C. After delipidation with organic solvents, a high concentration of organic acid (70% acetic or 60% formic acid) was used to solubilize the proteins for immediate HPLC analysis.

Size-exclusion chromatography mass spectrometry provides a rapid means with which to analyze purified membrane proteins such as the 12 transmembrane domain lactose permease (5). Fig. 1 depicts the results when this technique was applied to the components of the cytochrome *b₆f* complex. The absorbance and total ion chromatogram from mass spectrometry are shown for both spinach and *M. lamosus* (Fig. 1, A and B, respectively). The technique is very effective at separating protein components from more highly retained small molecule contaminants. Thus proteins elute first, providing a rapid overview (<15 min) of the components of the complex. The main limitation to the technique is chromatographic

resolution such that larger components (15–35 kDa) largely co-elute, generating complex overlapping ESI spectra that must be reconstructed to a zero-charge mass spectrum by appropriate software, effectively limiting the number of individual components that may be resolved by SEC-MS. The products of *petA–D*, as well as FNR in the spinach preparation, were detected in the reconstructed zero-charge spectrum, and their presence was confirmed by identifying genuine, unique ions for individual polypeptides in the original mass spectrum (Fig. 1C). The small subunits are quite well chromatographically resolved from the larger ones, although residual larger subunits can still be observed in the mass spectrum (Fig. 1D) and contribute to noise in the zero-charge reconstruction. Nevertheless, the four most prominent peaks in the reconstruction correspond to the four small subunits, confirmed by careful examination of the mass spectrum for the corresponding multiply charged ions (labeled in Fig. 1D *m/z* spectrum) and MALDI-TOF data (not shown). It is important to note that relative peak intensities are dependent upon abundance and ionization efficiency such that quantitation by this measurement is unreliable unless the latter is known. Cytochrome *b* has a quite low ionization efficiency and probably would have been regarded as insignificant in a blind analysis based upon SEC-MS alone. Consequently, analysis by a second technique, with greater chromatographic resolving power, was used for further definition of the complex.

Reverse-phase chromatography was combined with MS for a high resolution analysis of the complex (Fig. 2). While the chromatographic separation takes significantly longer, nearly all subunits are resolved in the experiment, allowing consideration of absorbance measurements for quantitation, although it should be noted that chromatographic elution efficiency³ is not 100% for all subunits. The addition of isopropanol to buffer B dramatically enhances the elution efficiency of many integral membrane proteins as reported originally (28), providing a viable alternative, in the case of the *b₆f* complex, to the solvent system containing 60% formic acid described previously (4). Most important was the ability to elute significant quantities of the cytochrome *b* polypeptide that transferred to the mobile phase at higher organic solvent concentrations close to the proteolipid PetN. The mass spectrum of cytochrome *b* illustrates the signal to noise (Fig. 2C). Zero-charge reconstructions are shown for all spinach subunits and display levels of heterogeneity typical for material stored for *short* periods at –80 °C (Fig. 2D). *M. lamosus* material also showed similar levels of heterogeneity (cytochrome *b* is shown) and no other subunits of significant abundance (see total ion chromatogram shown in Fig. 2B). The masses of the nine chloroplast and eight cyanobacterial subunits measured with ESI-MS are shown in Table I. In some

³ The percentage of a particular polypeptide population that elutes as the gradient passes the favored organic solvent concentration for transfer of that polypeptide from stationary to mobile phase.

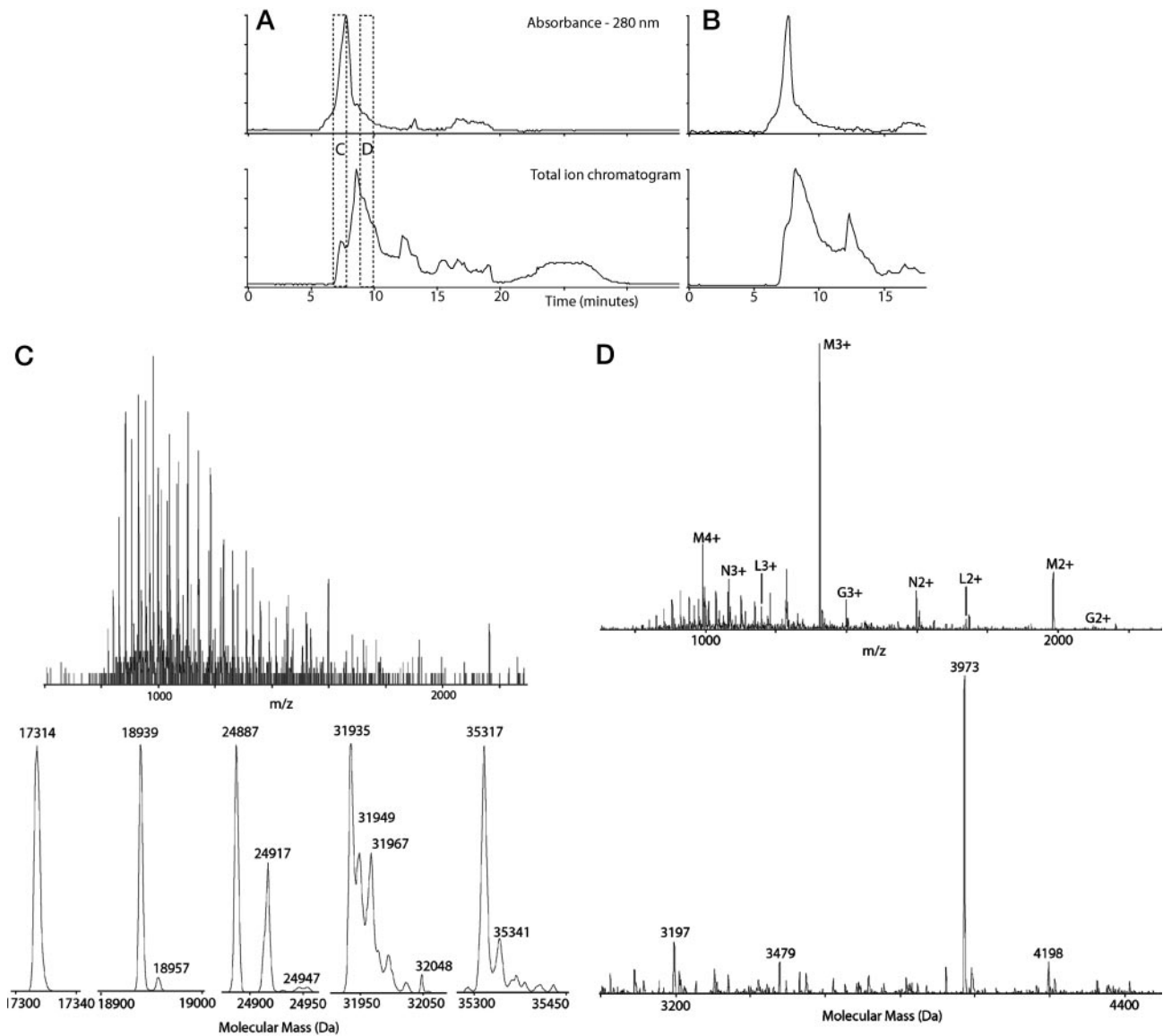


Fig. 1. Electrospray ionization mass spectra after size-exclusion chromatography (LCMS+) in aqueous organic solvents of subunits of cytochrome *b₆f* complex from spinach (A) and *M. laminosus* (B). Subunits (100 μ g of protein) precipitated with organic solvent (see “Experimental Procedures”) were dissolved in 60% formic acid prior to immediate injection onto a Super SW2000 size-exclusion column (4.6 \times 300 mm, Tosoh Biosep) equilibrated in chloroform/methanol/1% aqueous formic acid (4:4:1, v/v). Both $A_{280\text{ nm}}$ (upper panel) and total ion chromatogram (lower panel) are shown with full scale representing 100% relative intensity in each case. Peak absorbance for A was 750 milliabsorbance units and for B was 630 milliabsorbance units. The sum of ion intensities over the complete mass range (600–2300) is integrated in each scan (6 s) and plotted against time for the total ion chromatogram. Elution of protein components is complete by 15 min, and the later part of chromatogram B is omitted. Boxed C, spectra from region 1 correspond to large subunits. Boxed D, spectra from region 2 are dominated by small subunits. The y axes in all cases have arbitrary units. C, large subunits. The *m/z* spectrum is complex due to co-elution of the larger subunits (upper panel). Deconvolution of the *m/z* spectrum to generate the zero-charged molecular mass spectrum (BioMultiView 1.3.1) allowed identification of five large subunits, including PetD, PetC, cytochrome *b*, cytochrome *f*, and FNR (from left to right, lower panel). The *M. laminosus* preparation showed the presence of only the first four subunits (not shown). It should be noted that while strong signals were observed for cytochrome *f*, PetC, PetD, and FNR, where present, the relative ionization efficiency of cytochrome *b* was low such that in the zero-charge molecular mass spectrum shown it had \sim 1% of the intensity of that of cytochrome *f*. To distinguish the true cytochrome *b* signal from noise it was necessary to perform further experiments with reverse-phase chromatography to more thoroughly resolve cytochrome *b* (Fig. 2). D, small subunits. The SEC separation did allow for partial separation of small subunits with the spectrum still showing signal from larger proteins. While the four small subunits were the four strongest peaks in the reconstructed zero-charge spectrum (lower panel), the signals from larger proteins resulted in a quite noisy base line requiring careful examination of the appropriate ions in the mass spectrum, labeled in the upper panel (the letter used abbreviates the name of the subunit, and the number indicates the number of charges).

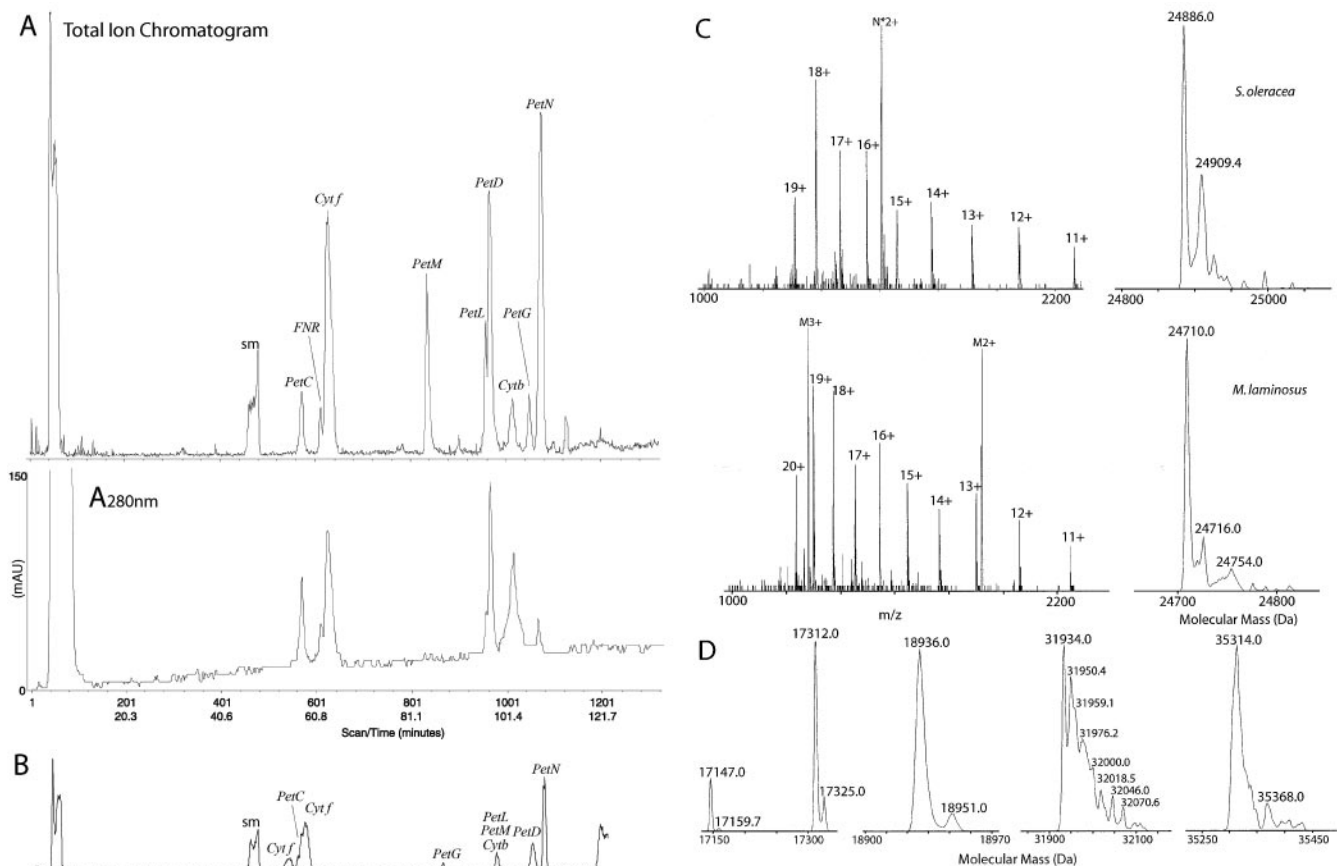


FIG. 2. Reverse-phase chromatography-mass spectrometry (LCMS+) of cytochrome b_6f complex subunits. A, total ion and $A_{280\text{ nm}}$ chromatograms of reverse-phase separation on 200 μg of protein of the spinach complex precipitated with 80% acetone and dissolved in 70% acetic acid prior to injection. Chromatography was in aqueous 0.1% trifluoroacetic acid eluted with acetonitrile/2-propanol (see "Experimental Procedures"). B, total ion chromatogram for the *M. laminosus* preparation. C, electro-spray ionization mass spectrum (m/z) and reconstructed zero-charge molecular mass spectrum of cytochrome b from spinach (upper panel) and *M. laminosus* (lower panel). Ions from co-eluting polypeptides are labeled according to their abbreviated identity and charge state (N^* refers to a singly oxidized, less retained form of PetN). D, reconstructed zero-charge molecular mass spectrum of the remaining spinach large subunits, PetD, PetC, cytochrome f , and FNR, respectively. *M. laminosus* subunits PetD, PetC, and cytochrome f showed similar levels of molecular heterogeneity. Significant quantities of FNR were only observed in spinach preparations. Fractions collected concomitant with the LCMS+ run provided highly enriched sources of each polypeptide for further analysis. sm, small molecules; Cyt, cytochrome.

cases the measured masses agree very well with masses calculated based upon annotated data base entries (Swiss-Prot). In spinach, FNR, PetC, and PetD are in good agreement ($<0.015\%$ deviation of measured versus calculated mass) with current entries, while greater uncertainties surround cytochrome f and cytochrome b as well as the cyanobacterial subunits that are less well characterized with respect to genomic sequence. In both species, cytochrome b showed the largest mass discrepancy even with the inclusion of a heme molecule in the theoretical mass calculation. Since it is thought that the two hemes associated with cytochrome b are non-covalently bound it is a possibility that one remains non-covalently associated during the ESI process, although this a rare observation under the conditions of sample preparation/ionization used. Alternatively a labile covalent modification should be considered, and we note the presence of a heme-staining band at 22 kDa that was observed in an original b_6f

preparation providing a precedent for a strongly bound heme on cytochrome b that is not dissociated during SDS-PAGE (29). Of course other modifications are possible, and the presence of approximately one chlorophyll a and one echinenone carotenoid per cytochrome b_6 subunit were reported recently (30). While the identities of the four large subunits were confirmed by peptide mass fingerprinting of CNBr-treated fractions from LCMS+ (see Supplemental Data), further analysis is underway to fully describe the primary structures of cytochromes f and b .

Toward the complete description of the subunits of the cytochrome b_6f complex, the small subunits were subjected to MSMS to generate sequence data. Fig. 3 depicts the result of selected MSMS experiments on PetL of spinach and PetG of *M. laminosus*. MSMS on intact parents was chosen because of the difficulties associated with recovery of trans-membrane domains after cleavage. In the case of spinach

TABLE I
Masses of spinach and *M. lamosus* cytochrome *b₆f* complex subunits by electrospray-ionization mass spectrometry

| Protein | Measured mass ^a | Calculated mass ^b | Modifications ^c |
|--------------------------|----------------------------|------------------------------|-------------------------------|
| | Da | Da | |
| <i>Spinacea oleracea</i> | | | |
| FNR | 35,313.9 ± 1.8 | 35,313.7 | |
| Cytochrome <i>f</i> | 31,934.7 ± 0.6 | 32,035.8 | 36–320, + heme |
| Cytochrome <i>b</i> | 24,886.9 ± 1.2 | 24,782.1 | + heme |
| PetC | 18,935.8 ± 0.3 | 18,938.6 | 69–247, + 1 disulfide |
| PetD | 17,311.8 ± 0.5 | 17,313.6 | Minus Met-1 |
| PetG | 4,197.5 ± 0.2 | 4,198.0 | <i>N</i> -Formyl |
| PetM | 3,971.9 ± 0.2 | 3,972.7 | |
| PetL | 3,477.8 ± 0.1 | 3,478.2 | <i>N</i> -Formyl, Ser-2 → Phe |
| PetN | 3,197.1 ± 0.4 | 3,197.8 | <i>N</i> -Formyl |
| <i>M. lamosus</i> | | | |
| Cytochrome <i>f</i> | 32,269.6 ± 3.3 | 32,269.4 | + heme |
| Cytochrome <i>b</i> | 24,709.6 ± 1.0 | 24,884.2 | + heme |
| PetC | 19,294.8 ± 1.6 | 19,202.8 | |
| PetD | 17,528.4 ± 0.5 | 17,521.9 | |
| PetG | 4,057.4 ± 0.2 | NA | <i>N</i> -Formyl |
| PetM | 3,841.0 ± 0.3 | 3,841.7 | |
| PetL | 3,530.4 ± 0.2 | 3,530.5 | <i>N</i> -Formyl |
| PetN | 3,303.6 ± 0.2 | 3,304.0 | <i>N</i> -Formyl |

^a Average mass, mean of three measurements to one decimal, ±S.D.

^b Calculated average mass based upon natural isotopic abundance and available sequence/modification data. NA, not available. The *M. lamosus* PetC and PetD masses are based upon the Nostoc sequence, which is regarded as most homologous.

^c Modifications include proteolytic removal of transit peptides (36–320 denotes removal of 1–35) or initiating methionine, *N*-formylation of the N terminus (retention of initiating formylmethionine), a discrepancy between published genomic translation and experimentally determined sequence and presence of heme.

PetL (Fig. 3A) a doubly charged parent was fragmented to produce singly charged daughters that corresponded to y3–y20 and b2–b13 providing overlapping sequence information for comparison with the sequence translated from the spinach chloroplast genome, in this case agreeing well except for the presence of Phe at position 2 (A CNBr experiment confirmed the presence of formyl-Met at position 1 (see Fig. 3 legend)). In the case of *M. lamosus* PetG (Fig. 3B) a triply charged parent ion was fragmented generating a wide range of fragments with one to three charges. The *inset* shows a triply charged daughter ion enlarged from the same mass spectrum illustrating the resolution obtained with hybrid quadrupole time-of-flight instruments allowing assignment of charge state, a great asset in interpretation of MSMS spectra from larger, multiply charged parent ions. In the absence of genomic data for *M. lamosus*, the spectra of the small subunits of this species were interpreted *de novo* with comparison to available sequences from other species. While the PetN, PetL, and PetM proteins could be fully assigned, the PetG sequence could be read only to position 29. Products of the spinach chloroplast genome, *petG*, *petL*, and *petN*, all retained their initiating formylmethionine, while the nuclear encoded *petM* product was cleaved after import from the cytoplasm (Table II). Interestingly, PetM from *M. lamosus* was the only small subunit from the cyanobacterium whose N terminus was not formylated despite being coded in the same genome as the other subunits (Table III). The sequences of the

chloroplast-encoded subunits were compared with translations of the recently available sequence of the spinach chloroplast genome (31). While the sequences of PetG and PetN revealed no discrepancy, Phe was detected at position 2 of PetL (raw data, MS-Product (prospector.ucsf.edu/) outputs for all eight small subunits and an annotated assignment of the spinach PetL data are provided in Supplemental Data). The spinach chloroplast genome reports a codon for Ser at position 2 implying the presence of either a DNA sequencing error or a previously undiscovered RNA editing event. The spinach PetM sequence shows a number of mainly conserved alterations when compared with the translated *Arabidopsis thaliana petM* sequence, and it is noted that while ChloroP (www.cbs.dtu.dk/services/ChloroP/) correctly identified the chloroplast location of PetM, the predicted N terminus was incorrect.

DISCUSSION

Obtaining full coverage of all protein classes is an important requirement for true proteomic studies, and some integral membrane proteins, especially larger ones with multiple transmembrane helices, present a unique challenge in this respect. While improvements in two-dimensional gel technology are addressing the problem (32, 33), the low accuracy and resolution of SDS-PAGE-determined molecular weights limit the value of this technique in intact mass proteomics. Intact mass measurements by ESI-MS provide mass accuracy, of-

FIG. 3. Sequence determination of small subunits of the cytochrome *b₆f* complex from spinach and the cyanobacterium *M. laminosus*. The sequences of spinach PetN, PetL, and PetG as well as *M. laminosus* PetN and PetG were determined by SEC-MSMS using a triple quadrupole mass spectrometer (API III, Applied Biosystems). **A**, MSMS spectrum of spinach PetL doubly charged parent (1740.2) showing y3–y20 and b2–b13 fragments (b8–b13 are labeled *b* for clarity; a full Excel table of assignments is provided in Supplemental Data) in agreement with the published gene sequence except for the presence of Phe instead of the reported Ser at position 2. To confirm the presence of formyl-Met at the N terminus (there was no b1 fragment detected) a sample from LCMS+ containing spinach PetL was treated with CNBr. The measured mass of the resulting product (3317.9405) confirmed removal of formyl-Met thus proving the presence of Phe in position 2 (see Supplemental Data). **B**, nano-electrospray MSMS was performed for the complete determination of spinach and *M. laminosus* PetM and the N-terminal 29-amino acid sequence of *M. laminosus* PetG. The MSMS spectrum shown was obtained by MSMS of the triply charged ion (1352.5) of PetG of *M. laminosus* in a fraction collected during LCMS+. Using the MSMS spectrum of both triply and quadruply charged parent ions it was possible to solve the primary structure of *M. laminosus* PetG from the N terminus to the 29th residue. The ion *inset* is from the MSMS spectrum of the triply charged parent ion illustrating the resolution achieved with a modern quadrupole time-of-flight instrument (Q-Star Pulsar, Applied Biosystems; nanospray source, Protana). This ion corresponds to y34³⁺, assuming the protein is 37 amino acids long. Interpretation of MSMS spectra was accomplished manually, aided by comparison of experimental data to all publicly available homologues aligned using ClustalW (npsa-pbil.ibcp.fr).

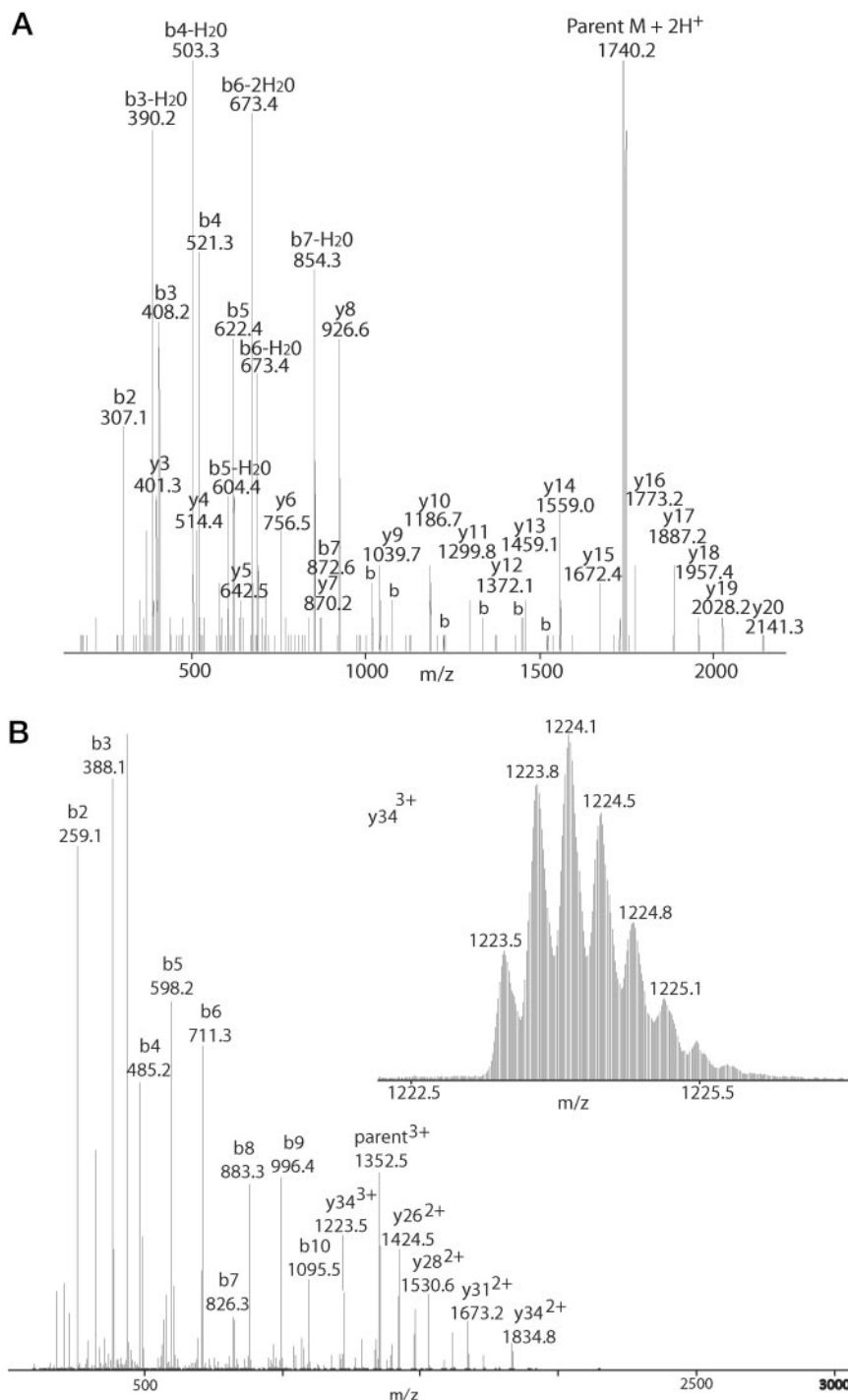


TABLE II
Amino acid sequence of spinach cytochrome *b₆f* complex small subunits determined by MSMS

| Subunit ^a | Sequence ^b | Mass (M + H ⁺) (calculated) ^b | Mass (M + H ⁺) (measured) ^c | Δ |
|-----------------------------------|--|---|---|------|
| | | | | ppm |
| PetG NP054954 | formylMIEVFLFGIV LGLIPITLAG LFVTAYLQYR RGDQLDL MIEVFLFGIV LGLIPITLAG LFVTAYLQYR RGDQLDL | 4196.3231 | 4196.3229 | 0.05 |
| PetM <i>A. thaliana</i> | NAAAEIFRIA AVMNGLTLVG VALGFVLLRI EATVEEAE NAVGEIFKIA AIMN AL TLVG VAVGFVLLRI ETSVEEAEAE | 3971.1680 | 3971.1803 | 3.10 |
| PetL NP054953 | formylMFTLTSYFGF LLAALTTISA LFIGLNKIRL I MSTLTSYFGF LLAALTTISA LFIGLNKIRL I | 3476.9635 | 3476.9727 | 2.65 |
| PetN NP054925 | formylMDIVSLAWAA LMVVFTFSL S LVVWGRSGL MDIVSLAWAA LMVVFTFSL S LVVWGRSGL | 3196.6943 | 3196.6746 | 6.19 |

^a Chloroplast-encoded subunits were compared to translations from the spinach chloroplast genome (31). PetM was compared to its *A. thaliana* homologue. Sequence disagreements are in bold. MSMS does not distinguish Ile and Leu so these are assigned by homology where possible.

^b Monoisotopic mass with no ¹³C.

^c High-resolution MALDI-TOF of first isotopic peak (zero ¹³C).

TABLE III
Sequences of *M. lamosus* cytochrome *b₆f* complex small subunits determined by MSMS

| Subunit ^a | Sequence | Mass (M + H ⁺) (calculated) ^b | Mass (M + H ⁺) (measured) ^c | Δ |
|----------------------|---|---|---|------|
| | | | | ppm |
| PetG ^d | formylMVEPLLDGLV LGLVFATLGG LFYAAYQQY... | NA ^d | 4056.226 | NA |
| PetM | MTEEMLYAAL LSFGLIFVGW GLGVLLKIQ GAEKE | 3840.074 | 3839.988 | 22.4 |
| PetL | formylMILGAVFYIV FIALFFGIIV GIIFAIKSIK LI | 3529.108 | 3529.056 | 14.7 |
| PetN | formylMEIDVLGWVA LLVVFTWSIA MVVWGRNGL | 3302.747 | 3302.489 | 78.1 |

^a Subunits identified by mass and sequence homology. MSMS does not distinguish Ile and Leu so these are assigned by homology where possible.

^b Monoisotopic mass with no ¹³C.

^c High-resolution MALDI-TOF of first isotopic peak (zero ¹³C).

^d NA, not applicable. PetG could not be sequenced beyond position 29 (see Supplemental Data).

greater proteome coverage, a return to simplified, purified protein complexes afforded improved detection of minor isoforms associated with dominant components. Thus, for detailed analysis of functional complexes, it is reasonable to subject them to individual analysis.

Size-exclusion and Reverse-phase Chromatography of Integral Membrane Proteins

A combination of size-exclusion and reverse-phase chromatographic separations allowed full subunit coverage analysis of the cytochrome *b₆f* complex from photosynthetic membranes of eukaryotes and prokaryotes, emphasizing both the advantages and disadvantages of these approaches. SEC provides a rapid overview of complex components, although chromatographic resolution is limited. Reverse-phase chromatography provides a more detailed look at individual components over the longer time course of the separation, although it is limited by reduced elution efficiency of specific components in 0.1% trifluoroacetic acid-containing buffers, in this case cytochrome *b₆*. This problem can be overcome by eluting the column a second time with 60% formic acid/isopropanol, as was necessary for efficient elution of the

larger PS2 subunits PsbA–D (8), and indeed such analyses confirmed the incomplete elution of cytochrome *b₆* in the primary separation (data not shown). The latter point is of note when UV measurements are used in quantitation.

Documentation/Discovery by ESI-MS of Additional Subunits in the Cytochrome *b₆f* Complex: FNR and Small Subunits

Before definitive mass spectral analysis, the presence of a fifth “large subunit” of the *b₆f* complex was controversial.

FNR (PetH)—The possibility of an additional FNR subunit in the spinach *b₆f* complex was first raised by Hind and coworkers (34) and was also noted by Hauska (35). However, gel electrophoresis provided definitive evidence for the presence in the complex of an active FNR in the spinach complex at apparently stoichiometric levels with important implications for the regulation of cyclic electron transport and the location in the photosynthetic membrane of the active site for NADP⁺ reduction mediated by photosystem I (17). FNR has not yet been detected in the complex isolated from the cyanobacterium *M. lamosus* (Figs. 1 and 2 above; Ref. 17) grown in the presence of normal (~0.1 M) salt concentrations. Under these

```

PETL_M.laminosus      -----MILGAVF ---YIVFIALFFGIA-- VGIIFAIKS---IKLI
PETL_ANAS P (Q8YVQ2)  -----MLAIVA ---YIGFLALFTGIA-- AGLLFGLRS---AKIL
PETL_CYAPA (P48102)  -----MVE ---YLVLSCMFGLA-- LACFFGLRS---IKLI
PETL_GUI TH (O78468)  -----MSLIIG ---YIILLACAFGLA-- AGLYFGLSA---IKLI
PETL_PORPU (P51221)  -----MSLFIG ---YIIFLVAFFGLA-- TGLFLGLKA---IKLI
PETL_ODOS I (P49524)  -----MTIAID ---YFLLVGFCFAFT-- SGLYLGLKS---IKLI
PETL_TOBA C (P12181)  -----MLTITS ---YFGFLAALTIT-- SALFIGLSK---IRLI
PETL_LOTJ A (Q9BBR4)  -----MPTITS ---YFGFLAVLTIT-- SGLFISLRK---LRLI
PETL_POPDE (Q02072)  -----MPTLTS ---YFGFLVALTIT-- LVLFIGLSK---IRLI
PETL_ARATH (P56776)  -----MPTITS ---YFGFLAALTIT-- SVLFIGLSK---IRLI
PETL_OENHO (Q9MTK4)  -----MLTITS ---YFGFLAALTIT-- SVLFIGLTK---IRLI
PETL_SPIO L (Q9M3L0)  -----MSTLTS ---YFGFLAALTIT-- SALFIGLNK---IRLI
PETL_BETV U (P46612)  -----MPTLTS ---YFGFLAALTIT-- SALFIGLNK---IRLI
PETL_WHEAT (P58247)  -----MLTITS ---YFGFLAALTIT-- PALFIGLNK---IRLI
PETL_MAIZ E (P19445)  -----MLTITS ---YFGFLAALTIT-- PALFIGLNK---IRLI
PETL_ORYS A (P12180)  -----MLTITS ---YFGFLAALTIT-- LALFIGLNK---IRLI
PETL_PINT H (P52805)  MKICI NHISFSPSTPTITIIIS ---YFGFLASIIFT-- LVLFISSK---IQLIQ NEGRGNPLSSLFQFQ
PETL_MARPO (P12179)  -----MLTIIS ---YFLFLIGALTLA-- LVLFIGLNK---IQLI
PETL_CHLRE (P50369)  -----MLTITS ---YVGLLIGALVFT-- LGIYLGLLKV--VKLI
PETL_CHLVU (P56306)  -----MVTIFS ---YIALLLSALVIT-- LTCYIGLLK---IKLI
PETL_NEPOL (Q9TKY9)  -----MFTVIS ---YFGFLVALAFT-- LVTYLG LRA---IQLI
PETL_MESV I (Q9MUN4)  -----MFTVVS ---YLGILAAAFALVT-- IGIPLVLR T---IQLI
    
```

FIG. 4. **Sequence alignment of available PetL sequences.** The experimentally determined *M. laminosus* PetL sequence was compared with other PetL sequences taken from the National Center for Biotechnology Information (NCBI) (July 4, 2002) using ClustalW (npsa-pbil.ibcp.fr). Note that the spinach gene sequence reports serine at position 2, while our experimentally determined sequence revealed phenylalanine at this position (Fig. 3 and Table II).

conditions, an FNR protein with a 9 kDa N-terminal extension is bound to the phycobilisomes (36). It has been suggested that in response to growth under high salt (~0.55 M) conditions, FNR binds to a different site in the thylakoid membrane (37).

It has been shown that FNR is functionally associated with the purified spinach cytochrome *b₆f* complex *in vitro* (17).⁴ Cytochrome *f* reduction by reduced ferredoxin/NADPH is inhibited by 2,5-dibromo-6-isopropyl-3-methyl-1,4-benzoquinone, and the half-time of the reduction is limited by the time (1–2 s) of conventional mixing in the spectrometer. Thus, the presence of FNR in the plant *b₆f* complex implies a significant physiological role of FNR in cyclic electron transport. The role of the *b* cytochromes in this pathway is not clear as their reduction by NADPH/ferredoxin is much slower than that of cytochrome *f* (38–40). This may be a result of the use of conditions that are not strictly anaerobic. It is not clear whether FNR is stoichiometric in all chloroplast *b₆f* preparations (35). Substoichiometric recovery of FNR might result due to loss of the subunit from the complex during isolation or substoichiometric association *in vivo*. While a role for FNR in cyclic electron transport is reasonable for *b₆f* in the stromal lamellae, this is not the case for *b₆f* in appressed membrane regions.

Another aspect of higher plant *b₆f* function that might be impacted by bound FNR is that of protein kinase regulation. Current models of kinase activation involve transmission of information regarding conformational status of the Rieske protein on the luminal side of the complex to the active site of the kinase on the stromal side via a conformational shift in the dimeric form of the *b₆f* complex (41). It has been proposed that peripheral proteins might modulate the behavior of the complex (42), and FNR would certainly be a candidate. Wor-

thy of discussion is the potential for FNR to provide an interface for communication of stromal reductant status to the *b₆f* complex and the kinase-modulated regulatory system. Such a regulatory role does not require that all complexes bind FNR but just that stromal ferredoxin/NADPH concentrations exert appropriate regulatory pressure at this control point. This contribution could be modulated by the amount of FNR expressed under different growth conditions and the abundance or status of other subunit proteins.

Small Subunits (PetG, PetL, PetM, and PetN)—After the original report of one to three acidic acetone-extractable small proteins <6 kDa (29) and the identification of the first small hydrophobic subunit in the *b₆f* complex of maize (43), four such small (molecular mass = 3.2–4.2 kDa) polypeptides, PetG, PetM, PetN, and PetL, have been found in the complex from higher plant (44) and cyanobacterial sources (44, 45) and more recently from *Chlamydomonas* (46). The function of these small subunits is unclear, although it is likely that the structural motif of each is a single transmembrane-spanning α -helix. Polypeptide subunits of this nature are not present in the cytochrome *bc₁* complex. Many such subunits have been found in the reaction center complexes of PS1 and PS2, and they may serve as a unique kind of integral membrane “hydrophobic filler” in photosynthetic membrane protein complexes (15) with critical roles in assembly and/or stability of the complex. It was reported that in *C. reinhardtii* photoautotrophic growth was impaired in the deletion mutant of *petG* (47) or *petL* (48) due to the dramatic decrease of the cytochrome *b₆f* level. A similar effect was observed in a *petN* deletion mutant in tobacco (49). Unlike the other three small subunits, *petM* is not essential for the assembly and function of the cytochrome *b₆f* complex in *Synechocystis* sp. PCC 6803 (50).

PetG, PetL, and PetN are chloroplast-encoded in higher plants and algae. However, PetM is a nuclear encoded gene product in the green alga *C. reinhardtii* (51) and in higher

⁴ H. Zhang and W. A. Cramer, in preparation.

plants (52). Sequence comparison shows a similarity of 52% (30% identity and 22% pseudo-identity) for PetG proteins (based on 29 sequences) and 56% (28% identity and 28% pseudo-identity) for PetN (based on 20 sequences). PetM is less conserved with a similarity of 29% (6% identity and 23% pseudo-identity based on 12 sequences). In PetL sequences, no conserved residue has been found, and there is only 19% pseudo-identity (based on 22 sequences). The sequences of the four small subunits from the *M. laminosus* *b₆f* complex have high similarity to those from the cyanobacterium *Nostoc* sp. PCC 7120. Fig. 4 shows the alignment of available PetL sequences including the *M. laminosus* sequence described here. The most conserved features appear to be a tyrosine residue at approximately position 6 and a basic residue approximately 4 residues from the C terminus. It is noted that two sequences display Phe in position 2 comparable to our observation of this residue at position 2 of the spinach protein.

There is not enough genome data accumulated so far to allow firm conclusions concerning conservation of the small polypeptide complement of the cyanobacterial *b₆f* complex. In the two cyanobacterial genomes completed thus far, *Nostoc* sp. PCC 7120 and *Synechocystis* sp. PCC 6803 contain genes for only three small subunits, *petG*, *petM*, and *petN* as annotated. However, the presence of PetL has been reported in *Synechocystis*, along with the other three small subunits (45), based upon mass spectrometric analysis of purified complexes. Blast searches have not yet allowed us to identify a *petL* homologue in *Synechocystis* sp. PCC 6803. Partial genome data for *Synechococcus* sp. PCC 7002 and 7942 show the presence of *petG* and *petM*, while the presence of *petL* and *petN* is not yet clear.

It is of significant interest that mass spectroscopic analysis has shown that the purified *b₆f* complex from spinach and the cyanobacterium *M. laminosus* contains all four of the small subunits including PetL. One may speculate that the presence of the PetL subunit in the *M. laminosus* complex is the reason that it is thus far the only cyanobacterium from which it has been possible to purify an active dimeric *b₆f* complex. The basis for this speculation is the finding that the absence of the PetL subunit in a mutant of *C. reinhardtii* destabilizes the active dimeric form of the complex in favor of the inactive monomer (53). A phosphorylated 15.2-kDa PetO subunit has been reported in a "gentle" preparation of the *C. reinhardtii* *b₆f* complex that did not include hydroxyapatite chromatography in the purification (54). PetO was not seen in another active preparation of active *C. reinhardtii* complex that includes this step (55) and has not been seen in any preparations of the complex from other sources including those from spinach or cyanobacteria. A 15.2-kDa component, as yet unidentified, was found in LCMS analysis of appressed thylakoid fractions (8), but homology searches in *A. thaliana* provide no evidence for a higher plant homologue of *petO*. No direct evidence for the presence of PetO in the preparations studied here has yet been obtained, but minor components, potentially represent-

ing weakly bound and non-stoichiometric subunits, are being investigated. A fifth small subunit of the cyanobacterial *b₆f* complex, PetP, has been proposed based upon MALDI-TOF analysis of purified complexes from *Synechocystis* sp. PCC 6803 that revealed an 8-kDa component (45). While we do detect a component of 8,117 Da in our *M. laminosus* preparations, when analyzed by reverse-phase LCMS+, the stoichiometry of the component is as yet unclear; the 8,117-Da component co-elutes with PetD negating the use of currently available absorbance data.

Rieske Isoforms (PetC)—The presence of three *petC* genes in *Synechocystis* sp. PCC 6803 (56) gives rise to potential isoforms of 18,996, 18,685, and 13,720 Da, while the only *petC* sequence available for *M. laminosus* has a theoretical molecular mass of 19,203 Da. The dominant component that we have assigned as PetC has a molecular mass of 19,295 Da (retention time, 57.2 min); minor components of 18,909 Da (54.4 min) and 14,800 Da (52.6 min) may represent *M. laminosus* PetC isoforms. While two-dimensional gel analysis of PetC in spinach suggested the presence of a second Rieske isoform, as is known for tobacco (25), we did not find any evidence for this species based upon mass spectral evidence. Either the isoforms are very similar in mass/retention, or the second isoform is expressed to a low, undetectable level. It is further noted that a single spontaneous asparagine to aspartate/isoaspartate conversion would alter the pI significantly while changing the mass by +1 Da only.

The difficulties discussed above highlight the need for improved quantitation in proteomics. A technique for more accurate identification and quantitation of minor isoforms based upon downstream analysis of fractions collected during LCMS+ is under development.

Acknowledgments—The Pasarow Family and the W. M. Keck Foundation are thanked for contributions toward instrument purchases. We thank Joseph A. Loo (UCLA) and Christie Hunter (Applied Biosystems) for assistance sequencing PetG (*M. laminosus*) and PetG and PetM (spinach) and K. F. Faull (UCLA) and J. Yan (Purdue) for helpful discussions.

* This work was supported by National Institutes of Health Grants AI-12601, AI-29733 (both to J. P. W.), and GM-38323 (to W. A. C.), Department of Energy Grant DE-FG03-01ER15251 (to J. P. W.), and the Henry Koffler Professorship (to W. A. C.). The costs of publication of this article were defrayed in part by the payment of page charges. This article must therefore be hereby marked "advertisement" in accordance with 18 U.S.C. Section 1734 solely to indicate this fact.

§ The on-line version of this article (available at <http://www.mcponline.org>) contains Supplemental Data.

§ To whom correspondence should be addressed: Dept. of Chemistry, UCLA, 405 Hilgard Ave., Los Angeles, CA 90095. Tel.: 310-794-5156; Fax: 310-206-2161; E-mail: jpw@chem.ucla.edu.

REFERENCES

1. Karas, M., and Hillenkamp, F. (1988) Laser desorption ionization of proteins with molecular masses exceeding 10,000 daltons. *Anal Chem.* **60**, 2299–2301
2. Fenn, J. B., Mann, M., Meng, C. K., Wong, S. F., and Whitehouse, C. M. (1989) Electrospray ionization for mass spectrometry of large biomol-

- ecules. *Science* **246**, 64–71
3. Chait, B. T., and Kent, S. B. (1992) Weighing naked proteins: practical, high-accuracy mass measurement of peptides and proteins. *Science* **257**, 1885–1894
 4. Whitelegge, J. P., Gundersen, C., and Faull, K. F. (1998) Electrospray-ionization mass spectrometry of intact intrinsic membrane proteins. *Protein Sci.* **7**, 1423–1430
 5. Whitelegge, J. P., le Coutre, J., Lee, J. C., Engel, C. K., Privé, G. G., Faull, K. F., and Kaback, H. R. (1999) Towards the bilayer proteome, electrospray-ionization mass spectrometry of large intact transmembrane proteins. *Proc. Natl. Acad. Sci. U. S. A.* **96**, 10695–10698
 6. le Coutre, J., Whitelegge, J. P., Gross, A., Turk, E., Wright, E. M., Kaback, H. R., and Faull, K. F. (2000) Proteomics on full-length membrane proteins using mass spectrometry. *Biochemistry* **39**, 4237–4242
 7. Turk, E., Kim, O., le Coutre, J., Whitelegge, J. P., Eskandari, S., Lam, J. T., Kreman, M., Zampighi, G., Faull, K. F., and Wright, E. M. (2000) Molecular characterization of *Vibrio parahaemolyticus* vSGLT. A model for sodium-coupled sugar cotransporters. *J. Biol. Chem.* **275**, 25711–25716
 8. Gómez, S., Nishio, J., Faull, K. F., and Whitelegge, J. P. (2002) The chloroplast grana proteome defined by intact mass measurements from liquid chromatography mass spectrometry. *Mol. Cell. Proteomics* **1**, 45–59
 9. Ghaim, J. B., Tsatsos, P. H., Katsonouri, A., Mitchell, D. M., Salcedo-Hernandez, R., and Gennis, R. B. (1997) Matrix-assisted laser desorption ionization mass spectrometry of membrane proteins: demonstration of a simple method to determine subunit molecular weights of hydrophobic subunits. *Biochim. Biophys. Acta* **1330**, 113–120
 10. Cadene, M., and Chait, B. T. (2000) A robust, detergent-friendly method for mass spectrometric analysis of integral membrane proteins. *Anal. Chem.* **72**, 5655–5658
 11. Musatov, A., and Robinson, N. C. (1994) Subunit analysis of bovine cytochrome bc₁ by reverse-phase HPLC and determination of the subunit molecular masses by electrospray ionization mass spectrometry. *Biochemistry* **33**, 10561–10567
 12. Whitelegge, J. P., Gómez, S. M., Stevens, R. L., Mastrogiacomo, A., Gundersen, C., and Faull, K. F. (1997) Electrospray-ionization mass spectrometry of lipidated intrinsic membrane proteins. *FASEB J.* **11**, A1088 (Abstr. 1357)
 13. Sharma, J., Panico, M., Barber, J., and Morris, H. R. (1997) Characterization of the low molecular weight photosystem II reaction center subunits and their light-induced modifications by mass spectrometry. *J. Biol. Chem.* **272**, 3935–3943
 14. Sharma, J., Panico, M., Barber, J., and Morris, H. R. (1997) Purification and determination of intact molecular mass by electrospray ionization mass spectrometry of the photosystem II reaction center subunits. *J. Biol. Chem.* **272**, 33153–33157
 15. Cramer, W. A., Soriano, G. M., Ponomarev, M., Huang, D., Zhang, H., Martinez, S. E., and Smith, J. L. (1996) Some new structural aspects and old controversies concerning the cytochrome *b₆f* complex of oxygenic photosynthesis. *Annu. Rev. Plant Physiol.* **47**, 477–508
 16. Widger, W. R., Cramer, W. A., Herrmann, R. G., and Trebst, A. (1984) Sequence homology and structural similarity between cytochrome b of mitochondrial complex III and the chloroplast *b₆-f* complex: position of the cytochrome b hemes in the membrane. *Proc. Natl. Acad. Sci. U. S. A.* **81**, 674–678
 17. Zhang, H., Whitelegge, J. P., and Cramer, W. A. (2001) Flavonucleotide: ferredoxin reductase is a subunit of the plant cytochrome *b₆f* complex. *J. Biol. Chem.* **276**, 38159–38165
 18. Mosser, G., Breyton, C., Olofsson, A., Popot, J. L., and Rigaud, J. L. (1997) Projection map of cytochrome *b₆f* complex at 8 Å resolution. *J. Biol. Chem.* **272**, 20263–20268
 19. Breyton, C. (2000) The cytochrome *b₆f* complex. Structural studies and comparison with the *bc₁* complex. *J. Biol. Chem.* **275**, 13195–13201
 20. Huang, D., Zhang, H., Soriano, G. M., Dahms, T. E. S., Krahn, J. M., Smith, J. L., and Cramer, W. A. (1999) in *Proceedings of the XIth International Congress on Photosynthesis* (Garab, G., and Pusztai, J., eds) pp. 1577–1580, Kluwer, Dordrecht, The Netherlands
 21. Martinez, S. E., Huang, D., Szczepaniak, A., Cramer, W. A., and Smith, J. L. (1994) Crystal structure of chloroplast cytochrome *f* reveals a novel cytochrome fold and unexpected heme ligation. *Structure* **2**, 95–105
 22. Zhang, H., Carrell, C. J., Huang D., Sled, V., Ohnishi, T., Smith, J. L., and Cramer, W. A. (1996) Characterization and crystallization of the lumen side domain of the chloroplast Rieske iron-sulfur protein. *J. Biol. Chem.* **271**, 31360–31366
 23. Carrell, C. J., Zhang, H., Cramer, W. A., and Smith, J. L. (1997) Biological identity and diversity in photosynthesis and respiration: structure of the lumen-side domain of the chloroplast Rieske protein. *Structure* **5**, 1613–1625
 24. Soriano, G. M., Smith, J. L., and Cramer, W. A. (2001) in *Handbook of Metalloproteins* (Weighardt, K., Huber, R., Poulos, T., and Messerschmidt, A., eds) Vol. 1, pp. 172–181, John Wiley & Sons, Chichester, UK
 25. Yu, S. G., Romanowska, E., Xue, Z. T., and Albertsson, P. A. (1994) Evidence for two different Rieske iron-sulfur proteins in the cytochrome *b₆f* complex of spinach chloroplast. *Biochim. Biophys. Acta* **1185**, 239–242
 26. Sainz, G., Carrell, C. J., Ponomarev, M. V., Soriano, G. M., Cramer, W. A., and Smith, J. L. (2000) Interruption of the internal water chain of cytochrome *f* impairs photosynthetic function. *Biochemistry* **39**, 9164–9173
 27. Wessel, D., and Flugge, U. I. (1984) A method for the quantitative recovery of protein in dilute solution in the presence of detergents and lipids. *Anal. Biochem.* **138**, 141–143
 28. Tarr, G. E., and Crabb, J. W. (1983) Reverse-phase high-performance liquid chromatography of hydrophobic proteins and fragments thereof. *Anal. Biochem.* **131**, 99–107
 29. Hurt, E., and Hauska, G. (1982) Identification of the polypeptides in the cytochrome *b₆f* complex from spinach chloroplasts with redox-center-carrying subunits. *J. Bioenerg. Biomembr.* **14**, 405–424
 30. Boronowsky, U., Wenk, S., Schneider, D., Jager, C., and Rogner, M. (2001) Isolation of membrane protein subunits in their native state: evidence for selective binding of chlorophyll and carotenoid to the *b₆* subunit of the cytochrome *b₆f* complex. *Biochim. Biophys. Acta* **1506**, 55–66
 31. Schmitz-Linneweber, C., Maier, R. M., Alcaraz, J. P., Cottet, A., Herrmann, R. G., and Mache, R. (2001) The plastid chromosome of spinach (*Spinacia oleracea*): complete nucleotide sequence and gene organization. *Plant Mol. Biol.* **45**, 307–315
 32. Molloy, M. P. (2000) Two-dimensional electrophoresis of membrane proteins using immobilized pH gradients. *Anal. Biochem.* **280**, 1–10
 33. Santoni, V., Molloy, M., and Rabilloud, T. (2000) Membrane proteins and proteomics: un amour impossible? *Electrophoresis* **21**, 1054–1070
 34. Clark, R. D., and Hind, G. (1983) Isolation of a five-polypeptide cytochrome *b-f* complex from spinach chloroplasts. *J. Biol. Chem.* **258**, 10348–10354
 35. Hurt, E., and Hauska, G. (1981) Cytochrome *f/b₆* complex of five polypeptides with plastoquinol-plastocyanin-oxidoreductase activity from spinach chloroplasts. *Eur. J. Biochem.* **117**, 591–599
 36. Schluchter, W. M., and Bryant, D. A. (1992) Molecular characterization of ferredoxin-NADP⁺ oxidoreductase in cyanobacteria: cloning and sequence of the *petH* gene of *Synechococcus* sp. PCC 7002 and studies on the gene product. *Biochemistry* **31**, 3092–3102
 37. van Thor, J. J., Jeanjean, R., Havaux, M., Sjollem, K. A., Joset, F., Hellingwerf, K. J., and Matthijs, H. C. (2000) Salt shock-inducible photosystem I cyclic electron transfer in *Synechocystis* PCC 6803 relies on binding of ferredoxin:NADP⁺ reductase to the thylakoid membranes via its CpcD phycobilisome-linker homologous N-terminal domain. *Biochim. Biophys. Acta* **1457**, 129–144
 38. Furbacher, P. N., Girvin, M. E., and Cramer, W. A. (1989) On the question of interheme electron transfer in the chloroplast cytochrome *b₆* in situ. *Biochemistry* **28**, 8990–8998
 39. O’Keefe, D. (1983) Sites of cytochrome *b-563* reduction, and the mode of action of DNP-INT and DBMIB in the chloroplast cytochrome *b-563/f* complex. *FEBS Lett.* **162**, 349–354
 40. Kramer, D. M. (1990). *Parallel Instrumentational Approaches to the Study of the Bioenergetics of Photosynthesis in Chloroplasts and Intact Plants*. Ph.D. thesis, University of Illinois
 41. Finazzi, G., Zito, F., Barbagallo, R. P., and Wollman, F. A. (2001) Contrasted effects of inhibitors of cytochrome *b₆f* complex on state transitions in *Chlamydomonas reinhardtii*. The role of Qo site occupancy in LHClI kinase activation. *J. Biol. Chem.* **276**, 9770–9774
 42. Wollman, F. A. (2001) State transitions reveal the dynamics and flexibility of the photosynthetic apparatus. *EMBO J.* **20**, 3623–3630
 43. Haley, J., and Bogorad, L. (1989) A 4-kDa maize chloroplast polypeptide associated with the cytochrome *b₆-f* complex: subunit 5, encoded by the

- chloroplast *petE* gene. *Proc. Natl. Acad. Sci. U. S. A.* **86**, 1534–1538
44. Whitelegge, J. P., Zhang, H, and Cramer, W. A. (2001) in *Proceedings of the 12th International Congress on Photosynthesis, Brisbane, August 18–23, 2001*, Abstr. S11-022, CSIRO Publishing, Collingwood, Victoria, Australia
 45. Schneider, D., Berry, S., Wenk S. O., Boronowsky, U., Jäger, C., de Weer, F. L., Dekker, J. P., and Rögner, M (2001) in *Proceedings of the 12th International Congress on Photosynthesis, Brisbane, August 18–23, 2001*, Abstr. S11-012, CSIRO Publishing, Collingwood, Victoria, Australia
 46. Zito, F., Vinh, J., Popot, J. L., and Finazzi, G. (2002) Chimeric fusions of subunit IV and PetL in the b_6f complex of *Chlamydomonas reinhardtii*. Structural implications and consequences on state transitions. *J. Biol. Chem.* **277**, 12446–12455
 47. Berthold, D. A., Schmidt, C. L., and Malkin, R. (1995) The deletion of *petG* in *Chlamydomonas reinhardtii* disrupts the cytochrome *bf* complex. *J. Biol. Chem.* **270**, 29293–29298
 48. Takahashi, Y., Rahire, M., Breyton, C., Popot, J. L., Joliet, P., and Rochaix, J. D. (1996) The chloroplast *ycf7* (*petL*) open reading frame of *Chlamydomonas reinhardtii* encodes a small functionally important subunit of the cytochrome b_6f complex. *EMBO J.* **15**, 3498–3506
 49. Hager, M., Biehler, K., Illerhaus, J., Ruf, S., and Bock, R. (1999) Targeted inactivation of the smallest plastid genome-encoded open reading frame reveals a novel and essential subunit of the cytochrome b_6f complex. *EMBO J.* **18**, 5834–5842
 50. Schneider, D., Berry, S., Rich, P., Seidler, A., and Rogner, M. (2001) A regulatory role of the PetM subunit in a cyanobacterial cytochrome b_6f complex. *J. Biol. Chem.* **276**, 16780–16785
 51. de Vitry, C., Breyton, C., Pierre, Y., and Popot, J. L. (1996) The 4-kDa nuclear-encoded PetM polypeptide of the chloroplast cytochrome b_6f complex. Nucleic acid and protein sequences, targeting signals, transmembrane topology. *J. Biol. Chem.* **271**, 10667–10671
 52. Kugler, M., Kruff, V., Schmitz, U. K., and Braun, H. P. (1998) Characterization of the PetM subunit of the b_6f complex from higher plants. *J. Plant Physiol.* **153**, 581–586
 53. Breyton, C., Tribet, C., Olive, J., Dubacq, J. P., and Popot, J. L. (1997) Dimer to monomer conversion of the cytochrome b_6f complex. Causes and consequences. *J. Biol. Chem.* **272**, 21892–21900
 54. Hamel, P., Olive, J., Pierre, Y., Wollman, F.-A., and de Vitry, C. (2000) A new subunit of cytochrome b_6f complex undergoes reversible phosphorylation upon state transition. *J. Biol. Chem.* **275**, 17072–17079
 55. Pierre, Y., Breyton, C., Kramer, D., and Popot, J.-L. (1995) Purification and characterization of the cytochrome b_6f complex from *Chlamydomonas reinhardtii*. *J. Biol. Chem.* **270**, 29342–29349
 56. Schneider, D., Skrzypczak, S., Anemüller, S., Schmidt, C. L., Seidler, A., and Rogner, M. (2002) Heterogeneous Rieske proteins in the cytochrome b_6f complex of *Synechocystis* PCC 6803. *J. Biol. Chem.* **277**, 10949–10954